Suppressing Current Deviations via the AC Skin Effect

A thesis submitted in partial fulfillment of the requirement
for the degree of Bachelor of Science with Honors in
Physics from the College of William and Mary in Virginia,

by

Sarah M. Sasinowska

Advisor: Prof. Seth A. Aubin

Prof. S. Mordijck

Prof. B. Castleberry

Williamsburg, Virginia
May 19 2025

Contents

Acknowledgments

Thank you to Professor Aubin for advising me and helping this project come to life; William, Trevor, and Russel, whose expertise never failed to guide me; Professor Mordijk for her aid in how to create and present a thesis; Will and Jonathon, who helped someone with two left hands design and craft a fantastic apparatus; Verona for being my best friend; and my parents, Heather and Chris, for their endless support and kindness through my college career.

List of Figures

List of Tables

Abstract

Magnetic fields allow us to control atoms; by manipulating a magnetic field induced via a current in a wire, one can force ultracold atoms to go where we want them to go. However, conductive defects in a wire trace severely impact the ability to generate a smooth current and magnetic field: a localized conductivity defect will produce an unwanted magnetic field defect. In contrast, at high frequencies, current tends to hug the edges of a conducting strip of metal due to the AC Skin Effect, reducing the impact of conductivity variations. This thesis describes an experiment to observe the suppression of a current deviation due to an engineered conductivity defect in a conducting strip of brass driven by an AC current at .25-5kHz. The AC current distribution in the strip is measured with a pick-up coil. Measurements of the current distribution reveal the presence of the current deviation and the AC skin effect. Numerical simulations of this setup predict a suppression of the current deviation. This thesis will experimentally prove the concept and principle of the AC Skin Effect by reducing the difference between the current density distribution of two metals joint side-by-side in the same ribbon-like wire.

Chapter 1

Motivation

Magnetic fields manipulate atoms, which is important for the construction of atom chips that make precise measurements. Electric currents create magnetic fields. If a wire, carrying the current that makes the magnetic field, has some form of conductive defect, then the magnetic field will vary at that location. Thus, the ultracold atoms will not be exactly where they need to be for the atom chip trap to make proper measurements. However, because of the AC Skin Effect, if the current is oscillating at a high enough frequency, the defect will not matter; the current will hug the 'skin,' or edge, of the wire. This has been proven in simulation, but it must be proven experimentally, in the lab. This thesis details the design and construction of an apparatus to measure the magnetic field deviation at high and low frequencies over a purposely constructed defective area. The distribution of the current is probed using an amplified pick-up coil to study the lateral AC Skin Effect. A pick-up coil detects current distribution by measuring the magnetic field caused by the current in the vicinity of the ribbon-like wire through the field's amplitude and phase. While the suppression of current deviations with the AC Skin Effect is an inherently interesting phenomenon on its own (involving the interplay of Ohm's Law and Faraday's Law), the broader motivation is to understand how this phenomena will impact ultracold atoms trapped in the vicinity of the microscopic wires of an atom chip.

1.1 The Atom Chip

By manipulating a magnetic field, one can control the position of atoms. If the current causing the magnetic field deviates, one cannot direct those atoms precisely or accurately. The deviations are unsatisfactory for making an atom chip with ultracold atoms, which uses currents to control the placement of the atoms. To better understand how to account for the variation of movement of atoms in the atom chip, it is pertinent to research how current flows through a defective strip of metal and how the resistivity and conductivity vary due to the defect.

Atom chips must have exactly placed atoms; they can produce Bose-Einstein condensates, degenerate Fermi gases, one-dimensional gases, and atom interferometers– simply put, they can make very precise measurements and create precise entities. Thus, the study of atom-surface interactions is far more difficult without atom chips. Prototypes for commercial applications of ultra-cold atoms utilize atom chips to trap the atoms and make very specific measurements [**1**].

In a traditional DC Zeeman (DCZ) atom chip, an external magnetic field B_{hold} cancels with the magnetic field from a wire carrying current I_z some distance from the wire and creating a minimum in the magnetic field. Rubidium atoms with the spin-up distinction seek weak fields, so they congregate to the area where the net field is weakest. However, there is a problem with the DCZ atom trap. If there are defects in the wire, there is deviation in the current of the DC Zeeman trap. The deviation carries into the magnetic field, resulting in the atoms conglomerating in clumps rather than a single unit (seen in Figure 1.1).

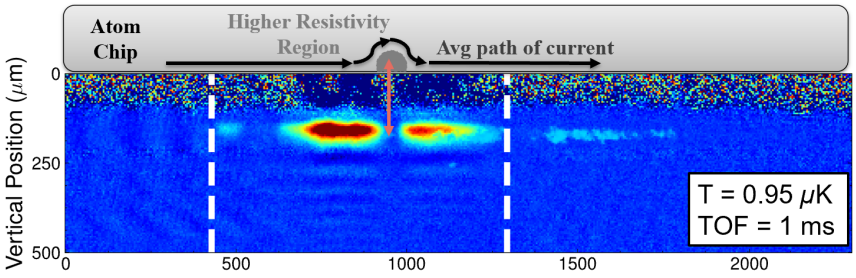

Figure 1.1: Trapped atoms found by William Miyahara. See the uneven clumping of the atoms; this clustering is due to a defect in the current-carrying wire.

Recently, a new type of atom chip trap has been invented that works using an alternating current (AC). The AC Zeeman (ACZ) trap has an alternating current I_z, but the magnetic fields function on a similar theory. The ACZ atom trap can trap both spin-up and spin-down Rubidium atoms.

An ACZ trap has the potential opportunity to suppress current deviations due to the conductivity defects via the AC Skin Effect, which states that at high frequencies, alternating currents hug the edges of their carrying wire. The AC Skin Effect works in simulation. However, in this thesis, it will be tested experimentally on a large ribbon-like wire by completing three tasks: simulating the apparatus with the purposely manufactured defects, creating a pick-up coil to read the current density distribution, and constructing the apparatus with the engineered conductive and resistive defects.

1.2 The AC Skin Effect

At high frequencies, current is pushed to the edges of the strip of its carrying wire; the effect is referred to as the Skin Effect. The Skin Effect, developed in the 19th century, primarily concerns the increase in alternating current (AC) resistance in relation to the effective decrease in cross-sectional area.

The current experiment's interest in the AC skin effect relates to a certain facet

of this theory: the lateral skin effect. This effect comes into play with a ribbon-like conductor, where the thickness is much smaller than the width or length. In the lateral skin effect, the current hugs the edges of the ribbon-like wire, no matter what defects lie in the wire. In the previous section, there is reference to how defects in the wire can cause deviations in current, which mean that the control of atoms is lost. However, according to the lateral Skin Effect, no matter if there is a resistive or conductive defect in the ribbon-like wire, the current will hug the edges at high frequencies. In a simulation by S. Du, there are resistive and conductive defects. At MHz frequencies, there is significant current deviation, but at GHz frequencies, there exists no visible variation [**2**]. Please see Figure 1.2 for visual aid.

1.3 Principle of Similitude

Because of the Law of Similitude, the Skin Effect acts the same at micro- and macro-scales, which is useful for the design and construction of scale-apparatuses. Much research on the subject of the AC Skin Effect simulates and models observables, like resistance, as a function of frequency or wave penetration depth [**1**]. The Principle of Similitude allows for the scaling of solutions to different sizes and frequencies and asserts that the distribution of the current (and thus, magnetic field) will be the same for the project's large scale metallic strip at a kHz frequency and for a 10s of microns wide atom chip at 5-10 GHz frequencies. What matters the most with this principle is the skin depth, or δm.

1.4 Structure of Thesis

]

The thesis shall be structured in the following manner:

Chapter 2 details the basic theory of the AC skin effect and the physics of the pick-up coil. It also contains information about the simulation of the apparatus, and what is expected in the experimental version. Chapter 3 describes the methodology and set-up of the experiment. It contains information on the construction of the apparatus and the testing of the apparatus's conductivity. It also details the plight of the construction of the pick-up coil. Chapter 4 presents the results of the current density distribution found across the apparatus. Chapter 5 contains the conclusion of the thesis and the outlook for future students or researchers who are interested in this physics.

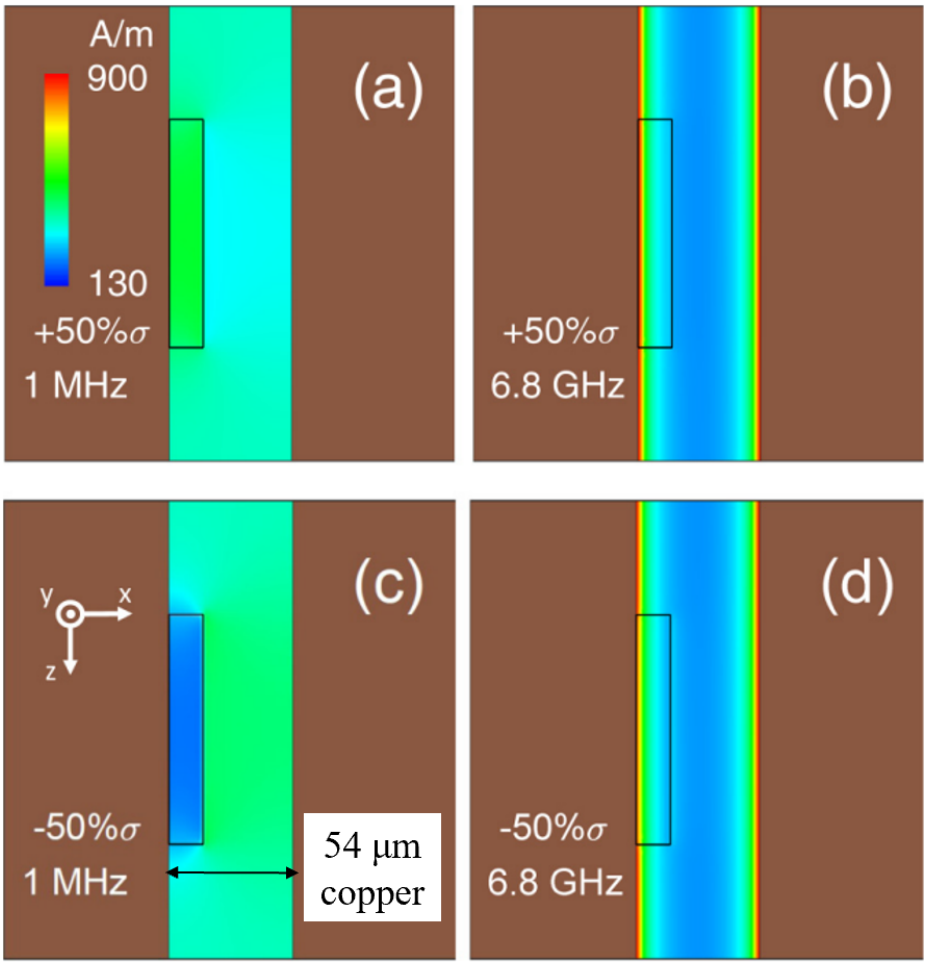

Figure 1.2: S. Du's simulation of the AC Skin effect over low and high frequency currents

Chapter 2

Mathematical equations and Theory

2.1 The AC Skin Effect Theory

Previous literature demonstrates the Lateral AC Skin Effect over a ribbon of aluminum [**1**]. Figure 2.1 shows the position versus amplitude of the magnetic field over several frequencies, with pink being highest frequency current and red being lowest frequency current, and the phase shift of the magnetic field across the width of the ribbon wire apparatus. One can see that, in simulation, at higher frequencies, the amplitude of the magnetic field is heightened at the edges of the ribbon wire.

As previously stated, defects in the atom chip wires cause deviation in the current's path at low frequencies. This is due to Ohm's Law, or $J = \sigma E$ with J being current density, σ being the conductivity of the material, and E being electric field. There is a direct relationship between current density and conductivity, so areas of high conductivity result in areas of high current density. However, this is only the case for currents at low frequency, as those currents can be assumed to be 'direct current' due to their low frequency.

For alternating current, one also must consider Faraday's law, which is time dependent. Faraday's Law is as follows:

$$\vec{\nabla} \times \vec{E} = -\frac{d\vec{B}}{dt} \tag{2.1}$$

in which the curl of the electric field ($\vec{\nabla} \times \vec{E}$) is equal to the negative time change of the magnetic field ($-\frac{d\vec{B}}{dt}$). To properly understand the flow of current at high frequencies, one must take the curl of Faraday's Law with Ampere's and Ohm's Law.

$$\nabla^2 J = \sigma\mu\frac{dJ}{dt} = i\sigma\mu\omega J = \frac{2i}{\delta^2}J \tag{2.2}$$

with σ being electric conductivity, J being the current density, μ being the magnetic permeability of the metal, ω being the frequency in radians/s, and δ being the skin depth, in meters. J is assumed to be the wave with equation $J(x) = Je^{i\omega t}$. The skin depth equation is found as follows:

$$\delta^2 = \frac{2}{\sigma\mu\omega} \tag{2.3}$$

with the same variables as mentioned before. As mentioned in Section 1.3, with the Principle of Similitude, so long as the skin depths are proportional to the frequencies, it does not matter how big or small the current-carrying wire is.

This proves that current flows to the edge of a ribbon-like wire. The current goes to the skin, and the size of that 'skin' can be determined with the above equation. In simple terms, at high frequencies, when you pit Ohm's Law against Faraday's Law, Faraday's Law wins! For a more pedagogical explanation of the Skin Effect, see [**1**]

2.2 The Pick-Up Coil Theory

In order to measure the current density distribution across the apparatus, a pick-up coil reads the magnetic field passing through the small area at the bottom

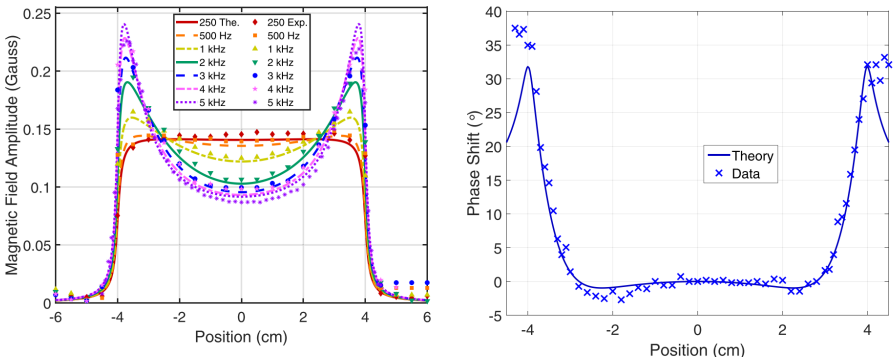

Figure 2.1: Annie Blackwell's figure that compares the data and theory for all measured frequencies

of the coil. By knowing the voltage in the wire, the area of the pick-up coil, and the magnetic field given by the pick-up coil, the calculation for the current density can be completed. An equation relating voltage, area, and magnetic field together is:

$$V_{coil} = -d/dt(\vec{A} \cdot \vec{B}) = -i\omega A B_x \tag{2.4}$$

which can be arranged in such a way in which the magnetic field, B_x relates to the current density $J(x)$,

$$V_{coil}(x) = -i\omega A B_x(x) \approx -i\omega A \frac{\mu_0}{2} J(x) \tag{2.5}$$

where ω is the frequency of the current in radians/second, μ_0 is the magnetic permeability of the metal, A is the area of the pick-up coil, V_{coil} is the voltage induced in the pick-up coil, B_x is the magnetic field through the x-direction of the pick-up coil, and $J(x)$ is the current density in the x-direction. Thus, the pick-up coil must be designed with as small an enclosed area as possible to gain the most accurate measurement of magnetic field. Figure 2.2 shows a not-to-scale design of the pick-up coil with reference lengths.

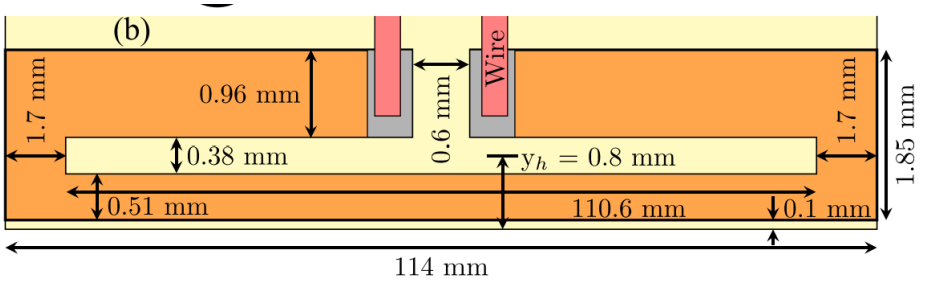

Figure 2.2: Annie Blackwell's not-to-scale design of the pickup coil

2.3 Simulation: AC Skin Effect vs Defect

Using CADFEKO simulation program, several diagnostic simulations were run. To ensure the simulation system was properly calibrated, the atom trap present in the Ultra-Cold Atom lab was constructed and simulated. With a coherent atom trap simulation completed, a simulation of an apparatus with no defect was designed. The non-defective simulation is just a bronze sheet of metal with current running through it. Once this appraisal run is properly running, the true simulation of the resistive and conductive defects can be completed.

With the following simulation settings, a seemingly correct outcome is received on CADFEKO v2024.1. This following set of instructions is for aid in running the simulation by oneself to duplicate the results seen below in Figures 2.3 and 2.6. The simulated apparatus has a length of 914 mm, a width of 100.16 mm, and a width of 0.503 mm. Constructed of 4 rectangles that are 'unioned', the apparatus exists in the N-plane. To give the different pieces of the apparatus the correct properties of the metal, the four-faced union is simulated via the Method of Moments (MoM), and three of the faces have the face medium of the brass for a thickness of 0.503 mm, with the meshing of 2. The final face is given the bronze medium with the same thickness and meshing. Thus, the total number of triangles for the meshing in the simulation is

47454. The simulation can be set at the different frequencies needed (250Hz-5kHz), and the configurations to be called is the flat near field.

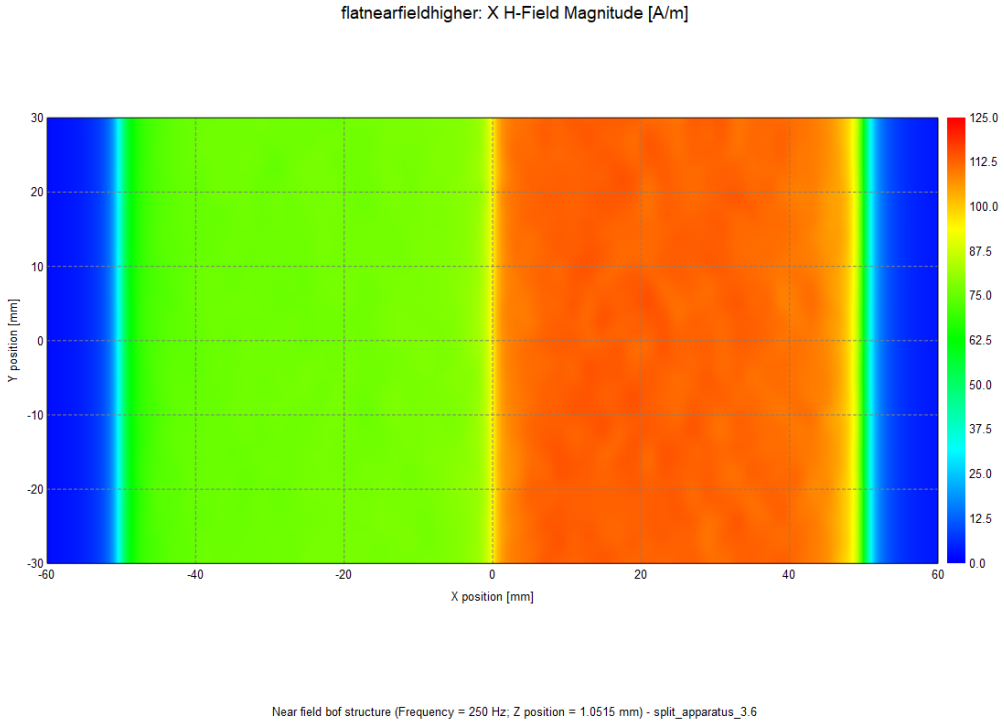

Figure 2.3: Simulation, focused on the center of apparatus, where the defect is. Here, the area of high current and low current density distribution can clearly be seen due to the current frequency being at 250 Hz.

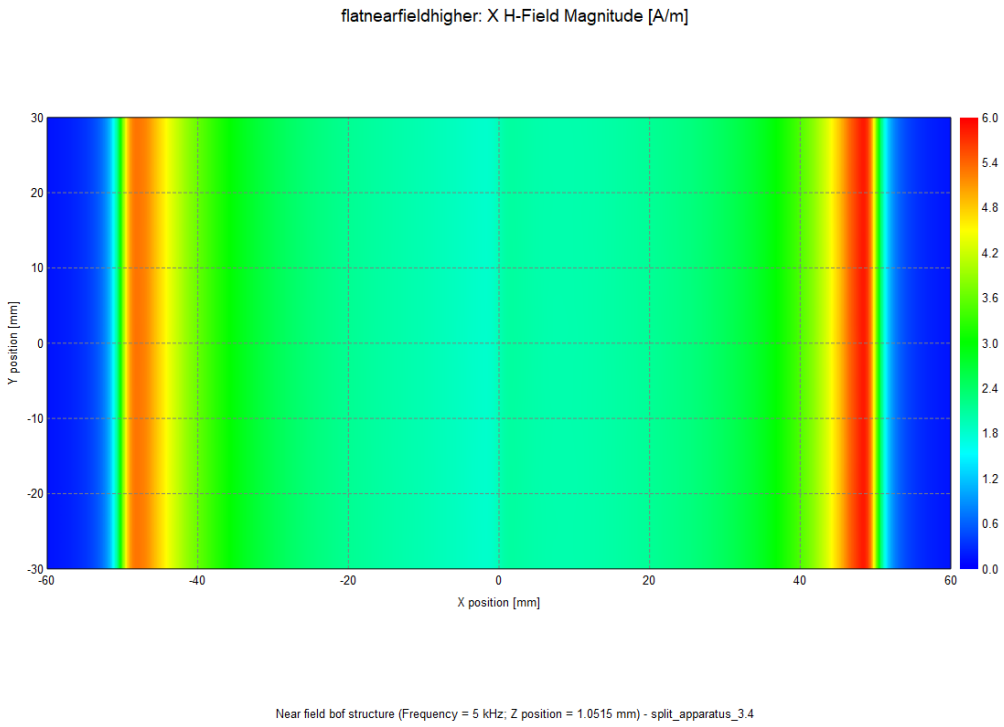

Figure 2.4: Simulation, focused on the center of apparatus, where the defect is. Here, the area of high current and low current density distribution cannot clearly be seen due to the current frequency being at 5 kHz.

Analyzing the results from the simulation gives the following graphs. By taking the average over the Y-position of the magnetic field magnitude and graphing them across the X-position, one can see the shape of the skin effect form. The following graphs, Figures 2.5 and **??**, utilize Equation 2.2 to show the current density distribution J(x) across the positions X and Y of the apparatus. By comparing the values of the maximums on the bronze and brass sides of the simulated apparatus in Table 2.3, one can see if the AC Skin Effect is effective in smoothing out deviations in the current distribution. However, note that the current density loses magnitude when at higher frequency in simulation. This phenomena was not seen experimentally, though, and is theorized to be a defect due to simulation. It is also worth noting that the simulation assumes the brass and bronze widths are equal, while in the experiment, the bronze

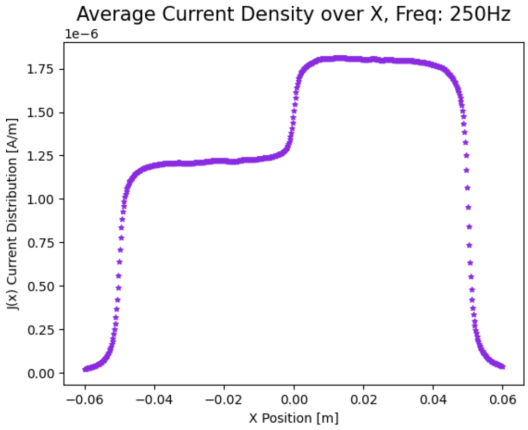

Figure 2.5: The current density distribution of the apparatus at 250 Hz. One can see the steep increase in current distribution where the conductivity is higher.

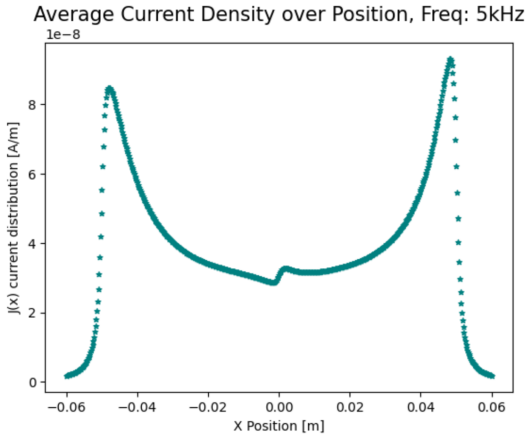

Figure 2.6: The current density distribution of the apparatus at 5 kHz. One can see the slight change in current distribution in the center of the plot, where the metal changes. However, the shift in the peaks is minimal despite the conductivity changes.

is a few millimeters longer wider than the brass. A more detailed simulation must be completed to entirely demonstrate the ability of the AC Skin Effect; however, this simulation does prove the concept does work and that the principle is sound.

Table 2.1: The results and analysis of the simulated graphs.

	Maximum Value Bronze	Maximum Value Brass	Ratio of Peaks
250 Hz	76.62	111.2	1.45
5 kHz	5.32	5.85	1.09

The difference of the ratios is 24.23%, which is significant enough to show that the AC Skin Effect works in theory–and that is should definitely be visible in experiment! With the theory of the AC Skin Effect and the pickup coil known, and the theory of the experiment successfully quantitatively produced via simulation, construction and experiment can be effectively begun.

Chapter 3

Apparatus

What separates this experiment from earlier demonstrations of the Lateral AC Skin Effect is the utilization of intentional defects in the ribbon wire. The experimental method probes the magnetic field's amplitude and phase at different current frequencies. The hypothesis states that at higher frequencies of current, the lateral skin effect will render the deviations caused by the defects infinitesimal. This develops a method of ensuring a consistent and reliable magnetic field for the atom chip's usage due to the Principle of Similitude.

The setup consists of a multi-centimeter wide sheet of metal that includes a cm-scale rectangular insert made from another metal with a much higher or lower conductivity—the defect (see Figure 3.1. A pickup coil will map out the amplitude and phase of the current distribution at kHz frequencies. Due to the Principle of Similitude, the skin depth will be proportional for the larger scale apparatus and the atom chip.

3.1 Construction of Apparatus

Meanwhile, several versions of the metal apparatus are under construction. Brass is the base metal, with two different types of bronze to be 50 percent higher and lower in conductivity. Each sheet of brass was cut three times. The first cuts

sliced the sheet in thirds, then the final cut sliced the center third vertically in half, so that the bronze ribbons could be inserted. Please reference Figure 3.2 for a visual aid in the cutting and construction of the apparatus.

To connect the brass sheets together, the method deemed best for fastening was milling halfway through the sheets on the edges and then using conductive glue to secure electrical coupling. First, acetone and a microfiber cloth clean an aluminum jig plate. The jig plate ensures the perpendicularity of the cuts and flatness of the sheet metal. Then, the sheet metal is affixed to the jig plate with double-sided sticky tape. Once all pre-cutting measures are taken, a high-precision drill press is zeroed to the height of the jig plate and sheet metal and lowered 3 millimeters. The drill press is then moved half of a millimeter into the sheet of metal. It cuts the metal down the side that is flush with the edge of the jig plate to ensure the parallel cut. For a close view of the cliff-edge, see Figure 3.3 Once the metal is manufactured, it is removed from the jig plate by gently prying it off with a pair of loose razor blades. Excess double-sided sticky tape is removed by lightly scraping with the razor blades or by washing with acetone.

When enough pieces are properly cut, they can be assembled with the conductive glue. The glue utilized here is MG Chemicals 8331D-A and -B. It is liberally spread on the edges of the both sheet metals to be affixed, then they are pushed together so that the milled edges overlap. A heavy weight (usually a jig plate, but once a large hammer was used) covered in wax paper is then placed atop the glued pieces. The weight ensures the glue is secure; the wax paper ensures that the glued pieces are easily pried from the weight. See Figure 3.4 to see two pieces after being glued together.

The glue sets for a day. Once dried, the weight is gently pried from the apparatus. Excess glue is scraped with a razor blade. The final step before measurements can

be taken is to connect wires to both ends of the ribbon-like wire apparatus. This is done by taking that razor blade and scratching small divots into the far sides of the apparatus so the glue has some friction to adhere to, and connecting the wire to the apparatus with conductive glue using the same methodology as repeated previously. When dried, a ribbon-like wire apparatus is ready for current density distribution measurement. See Figures 3.1 and 3.6 for the dimensions and design of the complete apparatus.

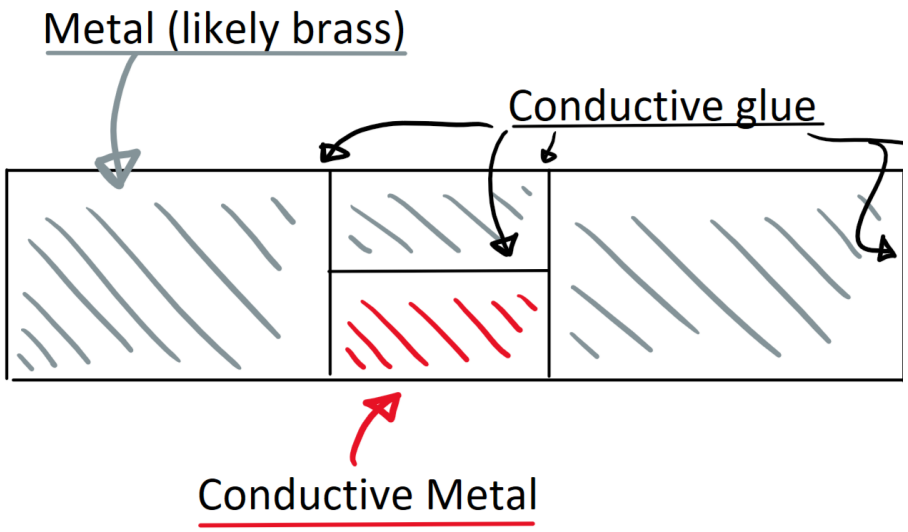

Figure 3.1: A crude design of apparatus

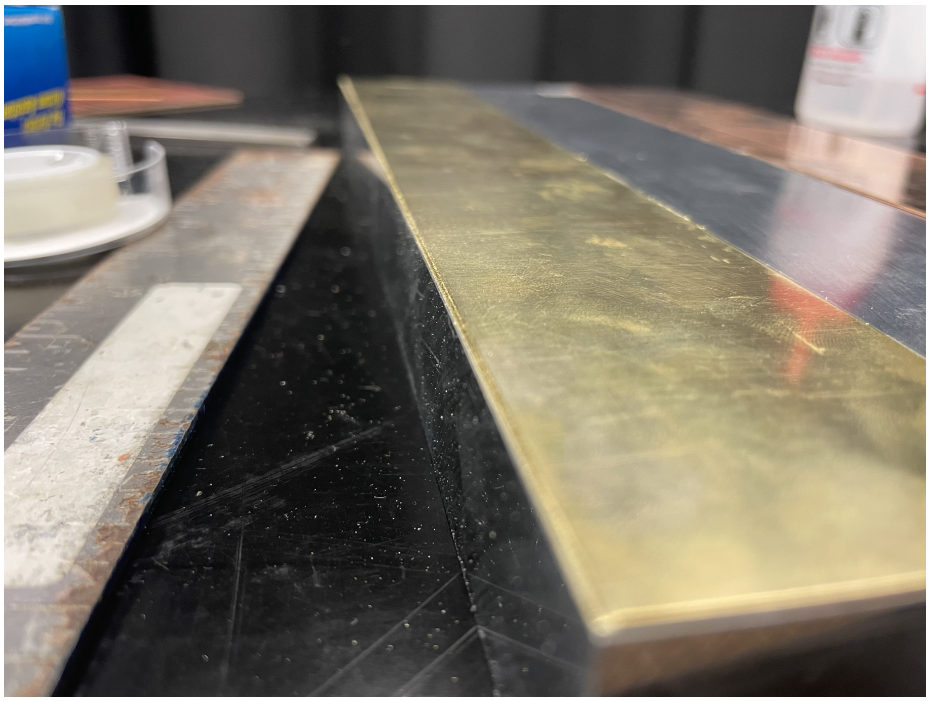

Figure 3.2: The milled edge of a piece of sheet metal.

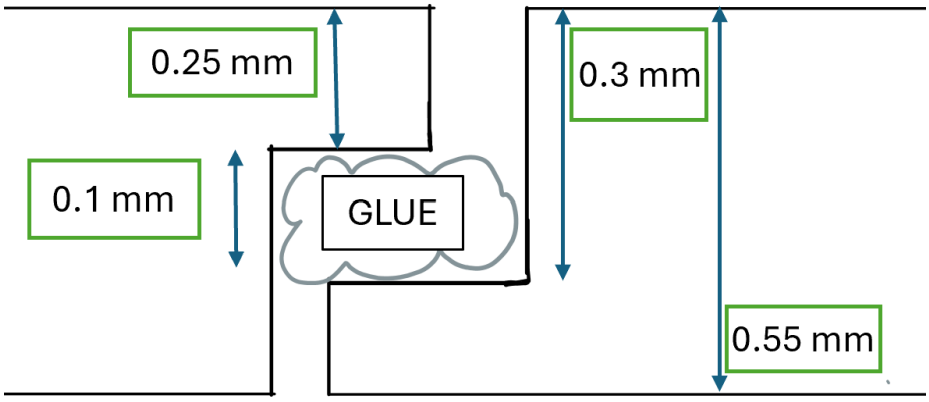

Figure 3.3: A figure with the measurements of the edges of the apparatus detailing how the different segments are glued together.

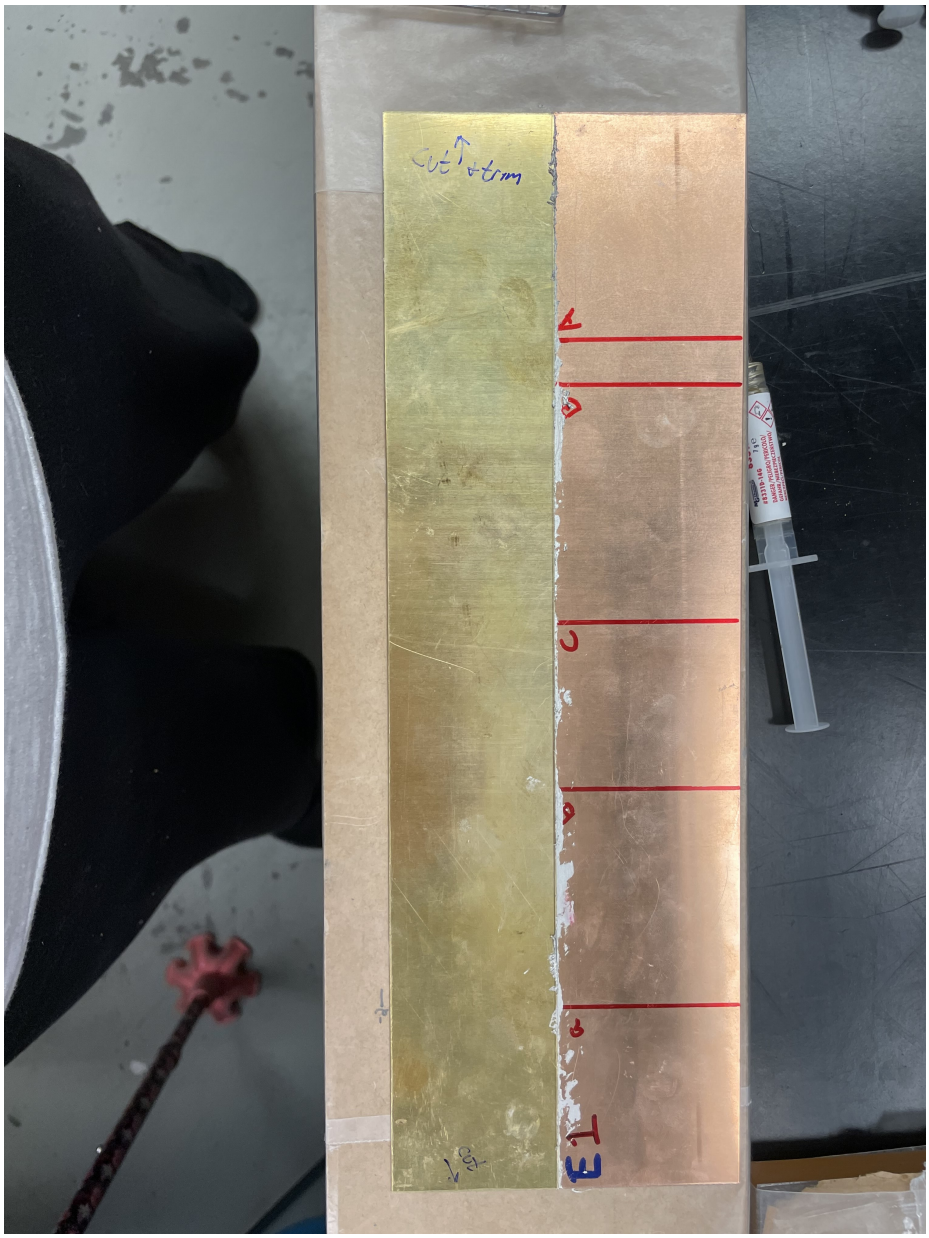

Figure 3.4: Two pieces of the apparatus glued together with the conductive glue.

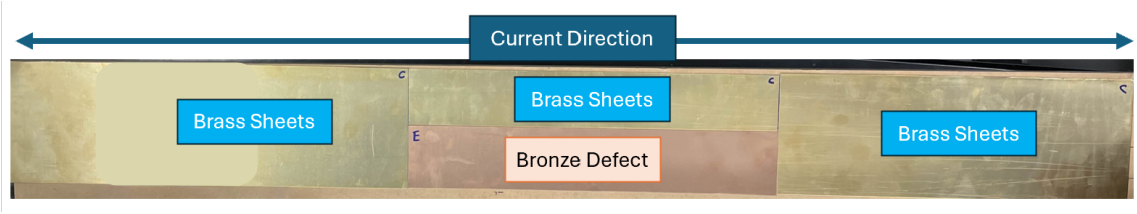

Figure 3.5: The apparatus cut into pieces but not yet glued together, with labels indicating the type of metal and the current direction.

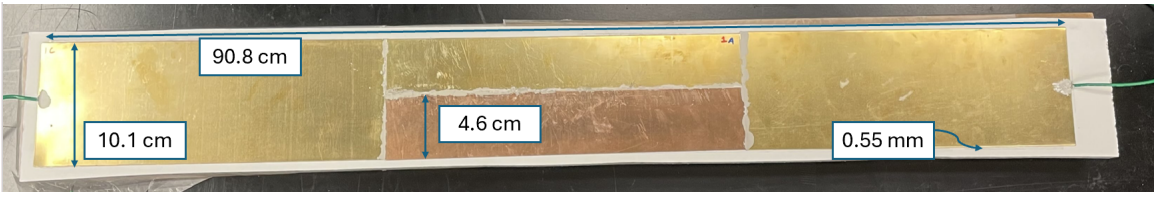

Figure 3.6: The glued together apparatus with the dimensions of the sides. See also the wires conductively glued at the far ends of the apparatus.

3.2 Measurement of Resistivity

To ensure that the brass and bronze have the correct resistivity as advertised on the McMaster-Carr website, a four-point measurement is taken. A current of 1.2 amps is sent through each piece before they are connected in the apparatus, and the voltage across the piece of metal is measured at different distances. See Figures 3.7 and 3.8 for the experimental setup. Once the voltages are taken and the distances measured, analysis for the exact resistivity may begin.

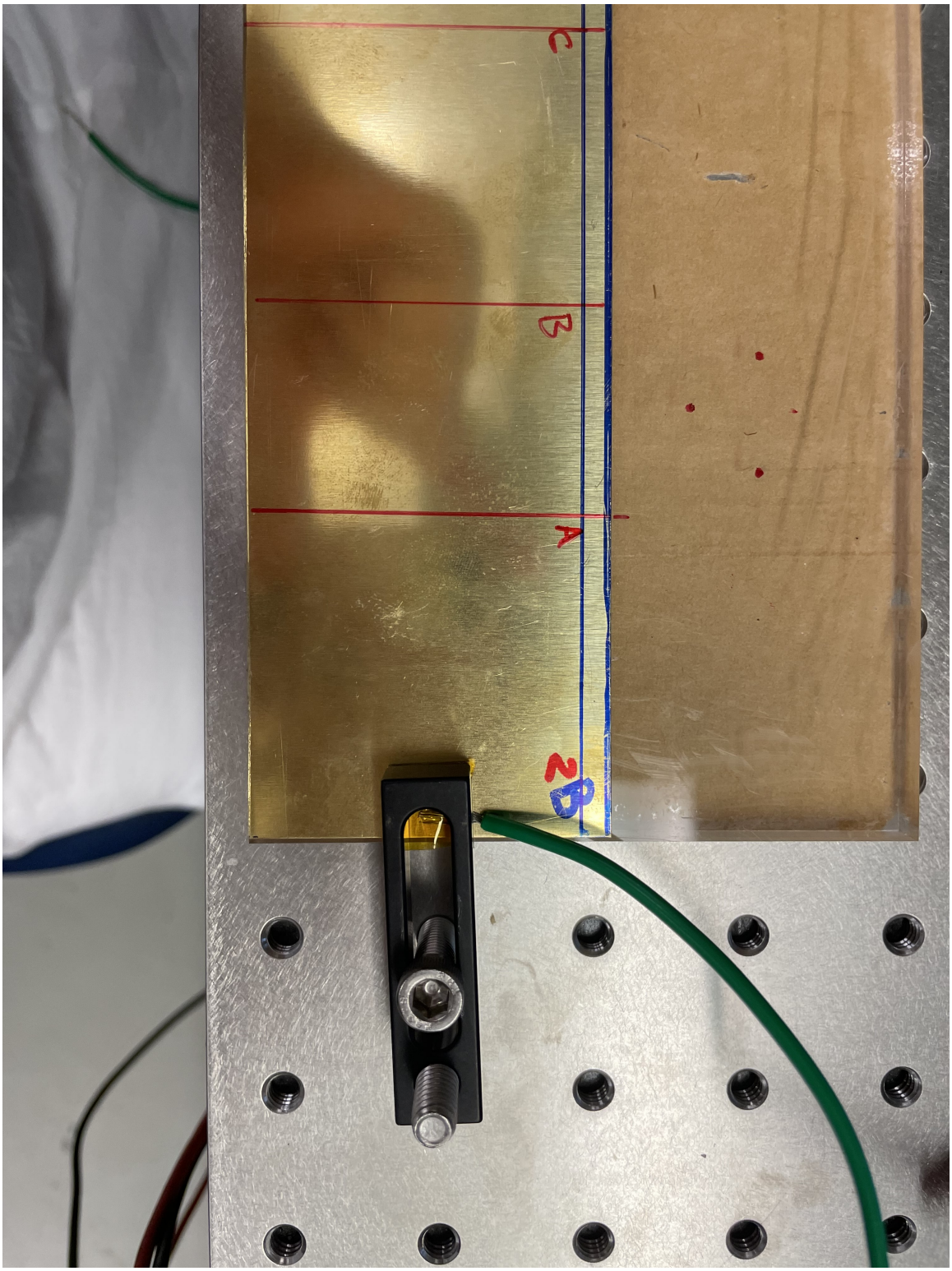

Figure 3.7: The experimental setup of taking resistivity measurements

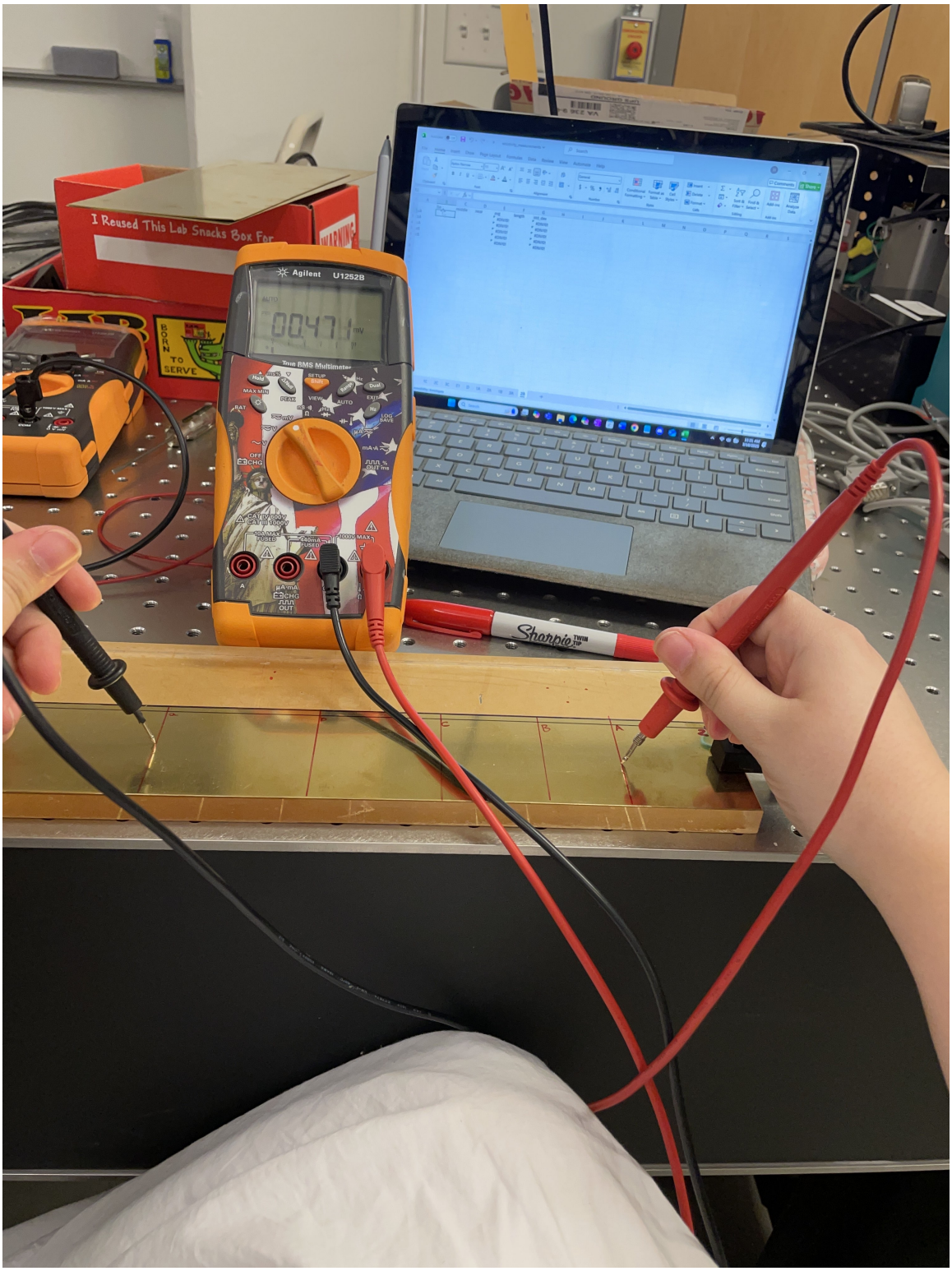

Figure 3.8: From the point of view of the data-taker, how the resistivity data was taken

Each of the three sheets brass are labeled A, B, or C. Then, each cut-up piece of brass is given a label 1, 2, 3, or 4. For example, an edge piece of brass could be labeled as '1B' or '4A'. After securing the sheet onto a block of plexiglass for electrical isolation, various distances are measured and drawn on the piece of metal. Conducting a four-point measurement, the current and voltage across two points of the metal are gathered. Along each parallel drawn line, three measurements of voltage are taken: two on the edges and one in the middle. These are then averaged and graphed with respect to the distance between the two voltage probes. An example of the graph for brass piece 3A is shown below (Figure 3.9).

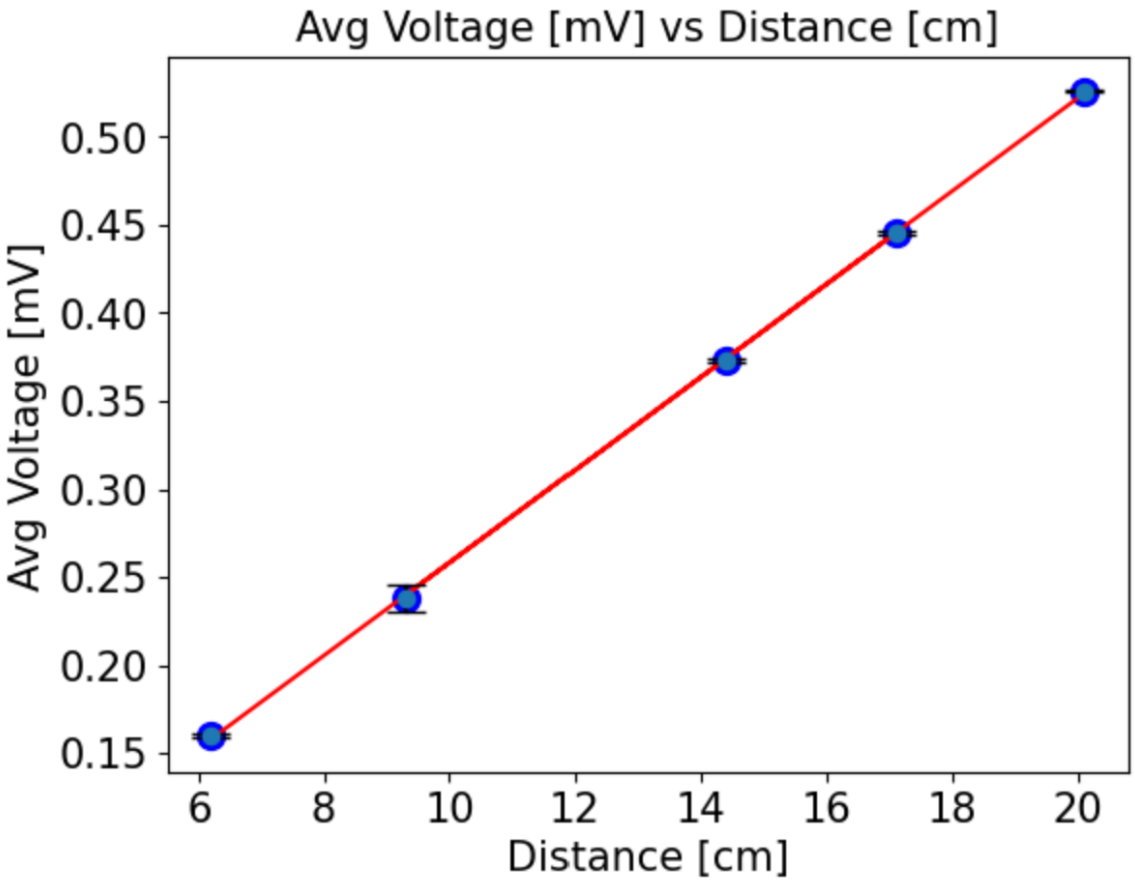

Figure 3.9: The graph comparing the average voltage across various lengths of the strip of brass labeled 3A

The slope of the line in Figure 3.9 is then divided by the area of that strip of brass (in this case, $5.4 * 10^{-2}$ m for width and $0.51 * 10^{-3}$ m for the thickness) to find the resistivity of $7.266 * 10^{-8}\Omega * m$. The rest of the resistivities for the sheets of brass can be found in Table 3.2. The original value given by the McMaster-Carr Website is $6.23 * 10^{-8}\Omega * m$.

Table 3.1: Resistivity of Brass. Error usually calculated by the standard deviation of the each voltage and the standard deviation on the curve fit parameters. For the average of all the resistivities, error is calculated over the standard deviation of all eleven values given.

Piece of Brass	Resistivity (x10ˆ-8) Ohm-meters	% Difference from given value	Error calculated by slope
1A	7.365	15.3	0.0095%
2A	7.448	16.3	0.079%
3A	7.266	14.2	0.017%
4A	7.199	13.4	0.038%
1B	7.422	16.0	0.03%
2B	7.528	17.2	0.33%
3B	7.447	16.3	0.33%
4B	7.243	13.9	0.039%
1C	7.325	14.9	0.019%
2C	7.257	14.1	0.027%
3C	7.439	16.2	0.0099%
Avg	7.351	1.24	9% [std dev]

The procedure and analysis for the two pieces of bronze are completed similarly. The McMaster-Carr resistivity value of 510 Bronze, or the resistive bronze, is $11.49\Omega * m$ and the value of 220 Bronze, or the conductive bronze, is $4.05\Omega * m$. As seen in Table 3.2, the difference from the McMaster-Carr values of bronze resistivity is minimal.

Table 3.2: The table of the resistivities of 510 Bronze and 220 Bronze, fashioned similarly to the table before.

Type of Metal	Resistivity (x10ˆ-8) Ohm-meters	% Difference from M-C value	% Difference from Brass	Error calculated by slope
Conductive Bronze	5.14	2.1	-21.29	0.019%
Resistive Bronze	11.18	2.7	47.08	0.052%

Chapter 4

Current Density Distribution

The last aspect of the project that needs completion is the construction of the pick-up coil, which will be used to read the amplitude and phase of the magnetic field of the ribbon wire. To construct the pick-up coil, the copper must be carved from a copper-clad printed circuit board (PCB) in a coil-like pattern. The coil must be very precise and very small in order to pick up the best readings for the magnetic field, so the making of the device must be done by machine. Despite the machine doing a lot of the work in carving off the copper, the machining process is tortuous. Many attempts were made at creating the pick-up coil, as will be detailed below.

However, once the pick-up coil exists, it is possible to probe the current density distribution of the apparatus. Qualitatively, one can see the sudden change of current at low frequencies and the high-to-low-to-high current at high frequencies. No exact numbers have been recorded yet.

4.1 Attempts of Construction of the Pick-up Coil

The first idea for the creation of the pick-up coil is using a Boss Laser. However, the Boss went down in September, and it could not be repaired for a very long time because the necessary parts were in a warehouse in Florida that was decimated by the hurricanes.

Another method was using a Computer Numerical Control (CNC) machine. Using a one-sided PCB, the CNC Carvey in the makerspace mills away the copper covering of the PCB to leave behind the specific shape of the coil. The copper shape will be on the bottom of the mostly-bare PCB, and two thin strips will go up the length of the pick-up coil. To mill the shape on the PCB, a larger mill bit (1/4" fishtail upcut bit) is used. When most of the board is stripped bare, a smaller, detail mill bit (1/32" fishtail upcut bit) drills off the millimeter-wide facets of the pick-up coil. Appendix A shows the code to design the milled pickup coil and Figure 2.2 from Chapter 2 is the enlarged image for viewing of the general shape. The attempts of making the pickup coil thus far can be seen in Figure 4.1. However, this method did not produce any good pick-up coils. Also, it eventually broke, as the mechanical button used for calibration stopped working. See Figures 4.2 and 4.3 for images and details of the broken Carvey.

Switching gears, attempts to construct a pick-up coil with the Triumph Laser are made. Although successful attempts of stripping the copper from the PCB occur, they were never consistent due to the copper being heated by the laser or the composition of the PCB. For attempts at producing consistent results, see Figures 4.4 and 4.5.

It is time to outsource the construction of the pick-up coil. A design is created in Eagle software, which produces a Gerber file. This file is sent to JLC PCB, who craft PCB circuitry based off costumer's files. With the professional PCB crafted (seen in Figure 4.6, measurements using the pick-up coil may be taken. Once the professionally carved circuitry arrives, work must still be done to create the pick-up coil. After careful examination of the PCB under a microscope to ensure quality and size, shown in Figures 4.7 and 4.8, the green plastic coating atop the copper is scraped off with a razor blade. Then, after scraping off the coating of a copper wire, the wire and the circuitry are soldered together. The copper wire then connects to a

Figure 4.1: the pickup coil attempts on the Carvey

secondary wire that has the ends that can connect to an amplifier for the collection of data. Figures 4.9 and 4.10 show the completed pick-up coil with the wires attached to the top and a piece of plexiglass attached to the back to aid in it standing alone. Figure 4.11 shows how the pick-up coil will read the magnetic field through the central area.

4.2 Probing for Current Density Distribution

With the apparatus constructed and the pick-up coil existing, the current density distribution can be probed experimentally. A function generator connects to a current generator. The current generator is hooked up to a resistor that controls the undesirable noise, and then it is connected to the apparatus. Above the apparatus

Figure 4.2: The broken Carvey during trouble-shooting. After investigation, it was found the calibration button was broken and needed replacement.

Figure 4.3: The broken Carvey button circuitry. The signal from the mechanical connection did not send to the rest of the circuit, making it impossible to close the circuit to properly calibrate.

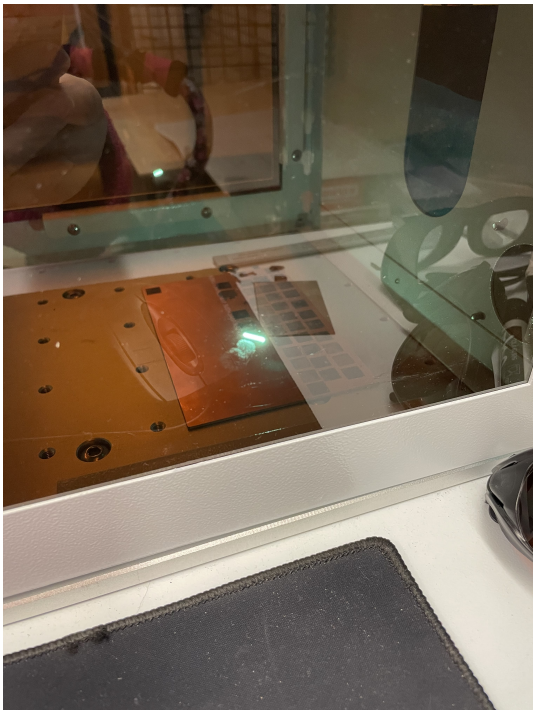

Figure 4.4: The Triumph laser cutting (and burning) into the PCB.

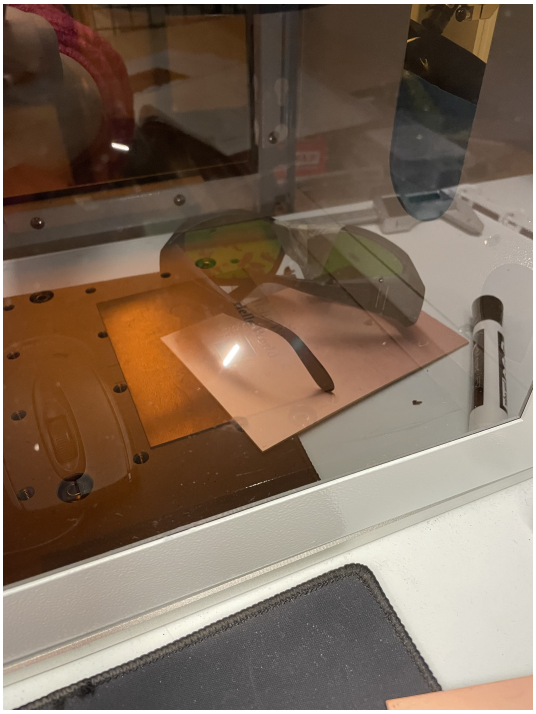

Figure 4.5: The Triumph laser cutting (and merely etching) into the PCB.

Figure 4.6: The PCB from JLC PCB before it was carved or wires soldered to it. The light green lines are the copper with a thin plastic coating overtop it.

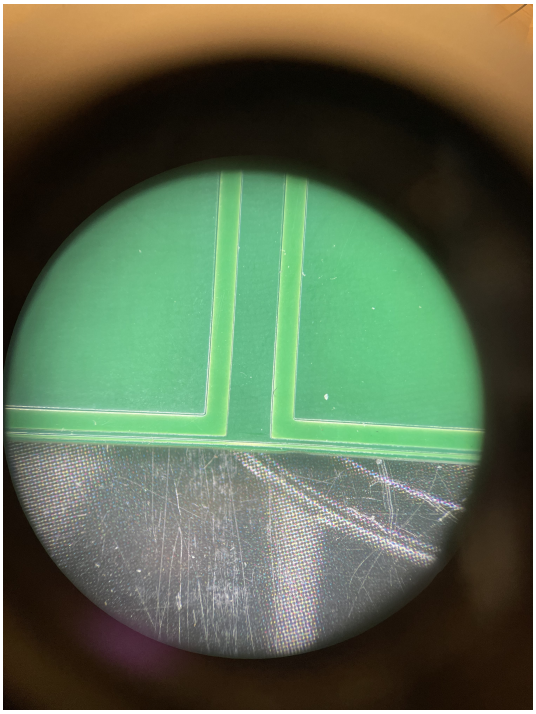

Figure 4.7: A view from the microscope at the center of the carved PCB

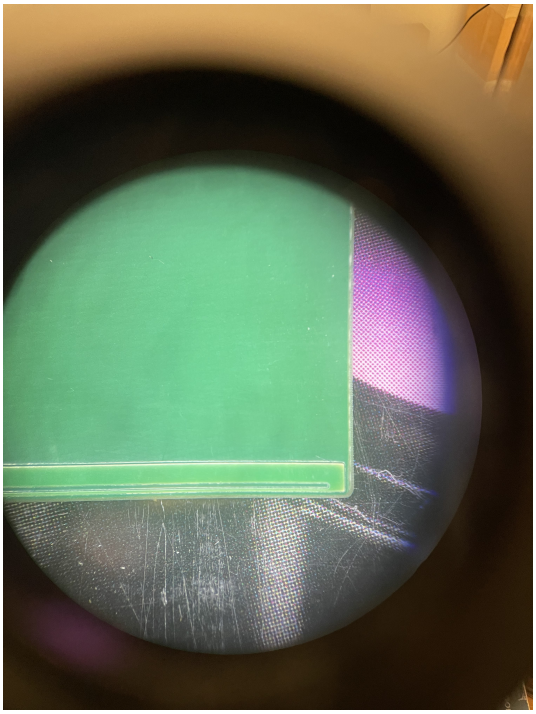

Figure 4.8: A view from the microscope at the corner of the carved PCB

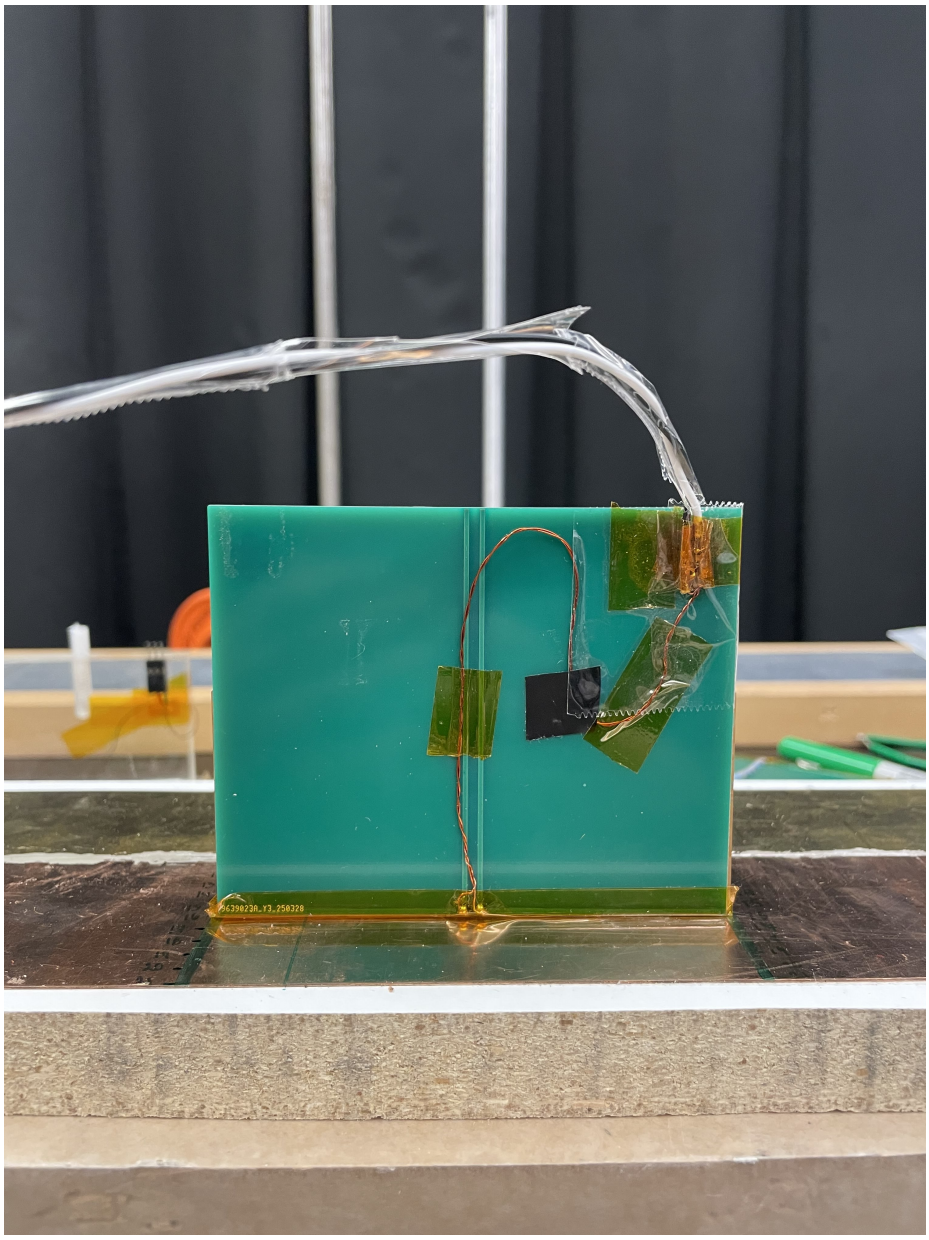

Figure 4.9: The completed pick-up coil, with the attached wires, standing atop the apparatus.

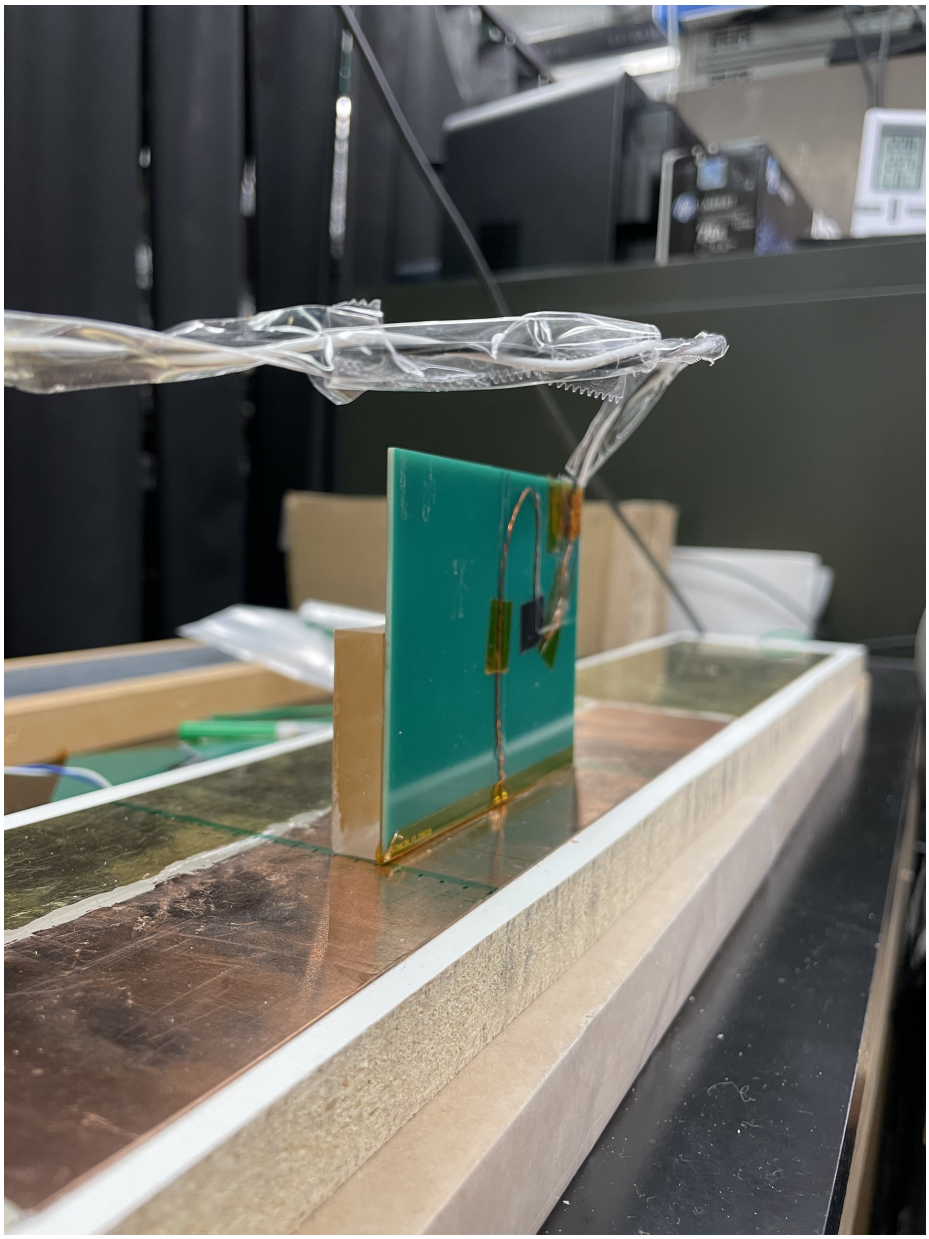

Figure 4.10: The completed pick-up coil, with block of plexiglass attached to the back to ensure it can stand upright.

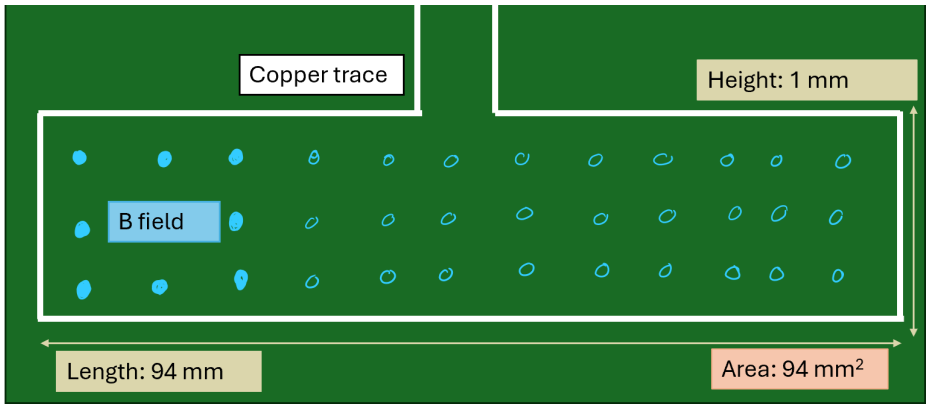

Figure 4.11: A graphic to explain the location of the B-field (magnetic field) and area used to find the current density distribution with the pick-up coil.

is an amplifier to which the pick-up coil connects (see Figure 4.12). The function generator, current generator, and pick-up coil output all attach to an oscilloscope (see Figure 4.13). For best results, most of these electronic components must be as far away from the apparatus as possible so there is minimal magnetic and electrical interference being caught by the pick-up coil.

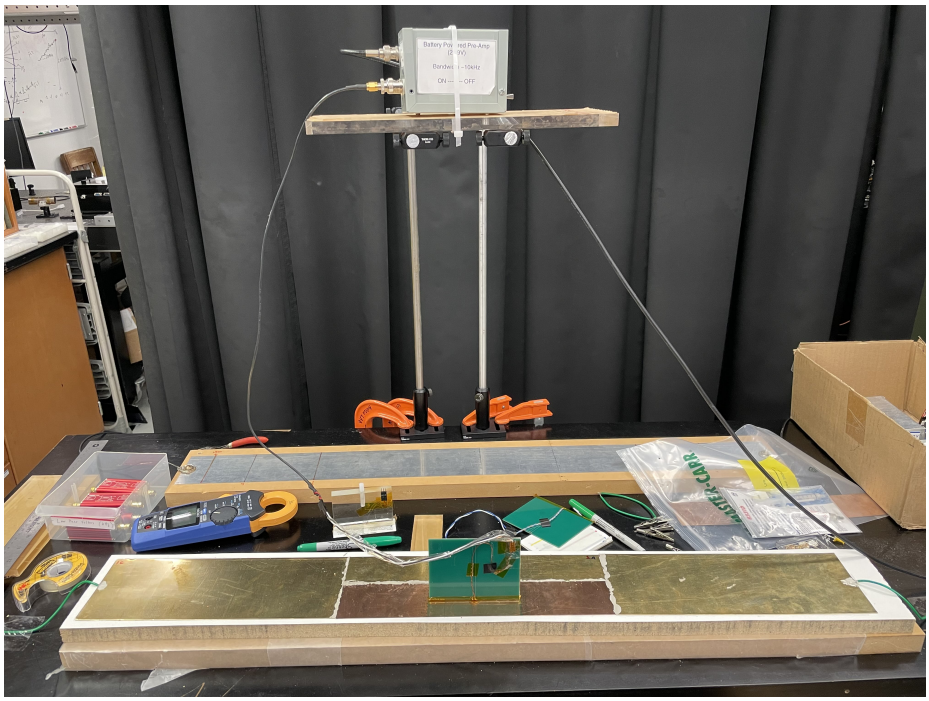

Figure 4.12: The apparatus on the table, the pickup coil sat atop the apparatus, and the amplifier floating above the pickup coil and apparatus.

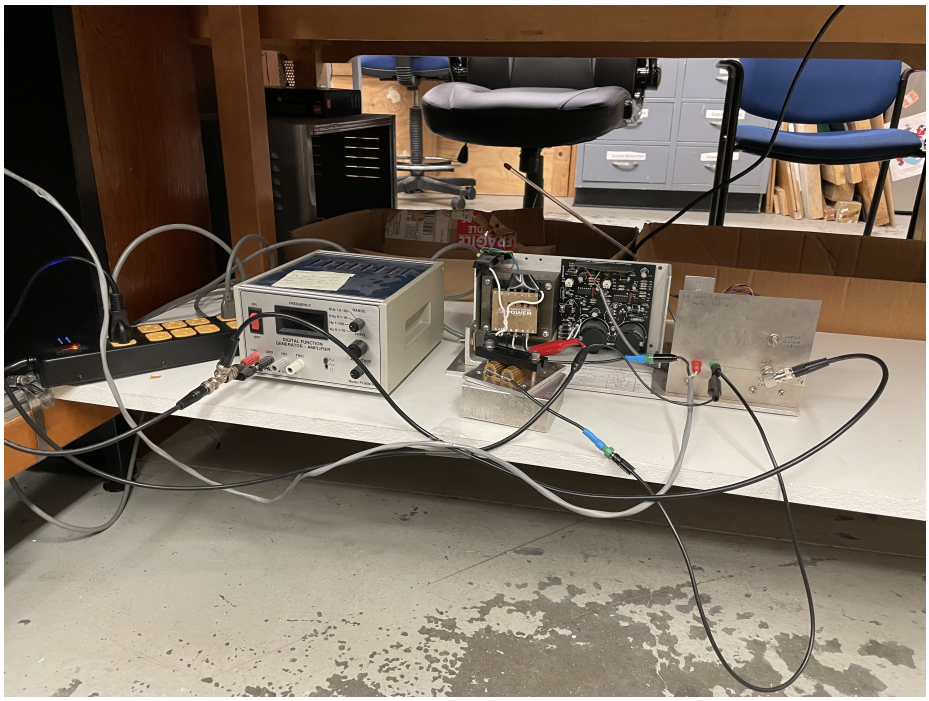

Figure 4.13: From left to right: the function generator and the current generator. The small box in front of the current genrator is the resistor.

While the current distribution is probed, the change in the voltage across the width of the apparatus is clear. At low frequencies, like 252 Hz, there is a mild drop off between the brass and the bronze being read from the scope. As seen in Figure 4.14, please note the triangular data set is a control data set–it is read on the same apparatus but where there is only brass. The triangular data is above the star-shaped data on the right side of the graph; this is because the bronze has a lower conductivity than the brass. However, at high frequencies, like 5025 Hz, one can see the rising of the signals near the edges and the lowering near the center, showing the AC Skin Effect in action! Please see Figure 4.15 to see the experimentally gathered data of the AC Skin Effect. Note, one side is higher than the other; this is due to the different materials' resistances. Because the brass is less resistive than the bronze, it has a higher peak for the current distribution. The ratio between the peaks for the 5 kHz

data is 1.13, and the ratio between peaks for the 250 Hz data is 1.40. This leads to a percent difference of 19.8% between the two frequencies. Compared to the the simulation's value of 24.23%, the percent difference between the frequencies is enough to be significant, confirming experimentally that the AC Skin Effect can be used to suppress current deviations.

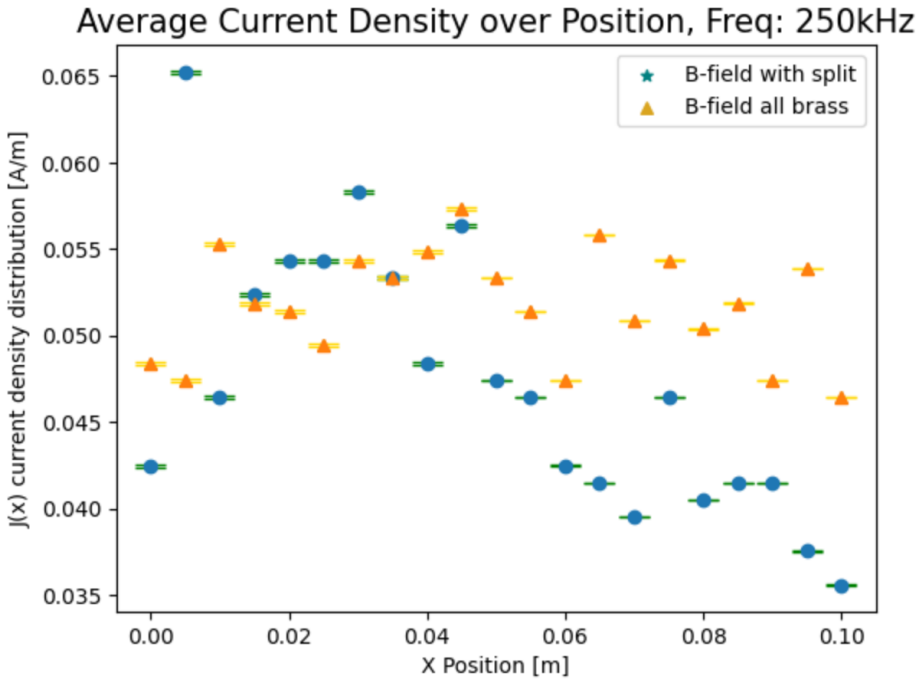

Figure 4.14: The current density distribution at 250 Hz. Brass only shown to help compare the step size of the brass-to-bronze current distribution.

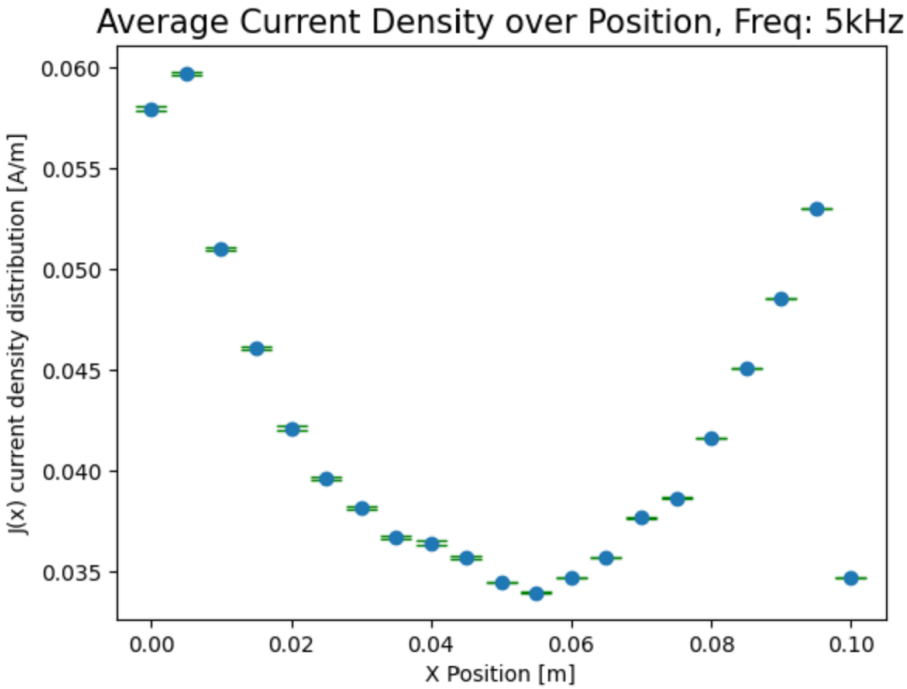

Figure 4.15: The current density distribution at 5 kHz.

Chapter 5

Conclusion

The AC Skin Effect is an experimentally sound theory, and it is proven that at higher frequencies, the current will more likely flow through a defective area of higher or lower resistance. After simulating and constructing an apparatus with an intentional defect and sending current through the apparatus at both low and high frequencies, by probing the magnetic field with a pick-up coil, the AC Skin Effect is shown to occur.

There are questions that open up after this project's completion, however. For example, there is the question of the phase of the current density. The input current from the function generator and output current read by the pick-up coil have different phases. What is that difference, and why does it occur? Is this a problem with the methodology that should be fixed or a result of the physics? There is also the question of the construction of the pick-up coil and its symmetry. The pick-up coil utilized in this thesis has only a fair symmetry, meaning it is similar when dragged across the metal back and forth, but it is not as ideally symmetric as desired. If this project were to be continued, the best place to start would definitely be in manufacturing a more symmetric pick-up coil. Also, if a future coil is to be made, the recommendation for continuing would be to make the top bit of copper thinner than the 0.6 mm I requested, as excess magnetic field may pass through the copper. If there are future

attempts at carving the coil oneself, be wary of the data sheets for the lasers in Small Hall's laser lab. The data sheets were frequently unreliable, inaccurate, and/or inaccessible.

The construction of the apparatus went much smoother than expected, however, which was a blessing, considering how difficult the pick-up coil was. Being able to construct the apparatus successfully using conductive glue and the cliff-like edges that fit together like a puzzle unexpectedly worked the first time trying it out. Although it took several heads being pressed together to figure out this method, it appears to be a reliable way to make the ribbon-like wire apparatus. If any apparatuses are constructed this way in the future, it would be interesting to see if making the cliff depths wider – say, a whole millimeter – would have any effect on the physical connection or signal.

This project overall aided in the learning of simulation, experimental construction, and data gathering and analysis, which are incredible skills to have gathered during a senior thesis and will prove most useful in the continuation of a scientific career.

Appendix A

HTML code for the pick-up coil

<html>

<svg width="200" height="200" viewBox="-150 -150 200 200">

<polygon points'"-100,-100 -100,-98.15 14,-98.15 14,-100 -42.4,-100 -42.4,-99.04 12.6, -99.04 12.6,-98.24 -98.24 -98,-98.24 -98,-99.49 -43,-99.04 -43,-100" fill="none" stroke="#000000" stroke-width=".1"/>

<polygon points="-102,-102 -102,-96 15,-96 15,-102" fill="none" stroke="#000000" stroke-width=".1"/>

< /svg>

<html>

Appendix B

Python Code for Data Analysis

For Experimentally Gathered Data from Apparatus:

```
x_direction = []

voltage= []

omega = 31573

mu = 4*3.1415*10**-7

Area = .00000324

B_field = []

for value in voltage:

    B = (value * 2 )/(omega * mu * Area)

    B_field.append(B)


J_x = []

for value in B_field:

    j = value*2/(4*3.14*(10**7))

    J_x.append(j)


plt.title('Average Current Density over Position, Freq: 5kHz', fontsize=15)

plt.scatter(x_direction, J_x, color='teal',s=15, marker='*',label="b field")
```

```
plt.xlabel('X Position [m]')
plt.ylabel('J(x) current density distribution [A/m2]')
plt.show()
```

For Simulated Data in a .dat file:

```
#empty lists
x_direction = []
z_direction = []
B_field = []

#load the file
tempdata = []
tempdata = np.loadtxt('[.DAT FILE]', usecols=(0,1,2), dtype=str)
x_direction.append(tempdata[:,0])
z_direction.append(tempdata[:,1])
B_field.append(tempdata[:,2])

#makes the lists numbers
x_direction_ = np.array(np.concatenate(x_direction), dtype=np.float64)
z_direction_ = np.array(np.concatenate(z_direction), dtype=np.float64)
B_field_ = np.array(np.concatenate(B_field), dtype=np.float64)

#average the x-positions and B-fields over the z-position
x_avg_5 = []
b_avg_5 = []
z_avg_5 = []
```

```
x_groups = [x_direction_[x_direction_ == i] for i in np.unique(x_direction_)]
b_groups = [B_field_[x_direction_ == i] for i in np.unique(x_direction_)]
z_groups = [z_direction_[x_direction_ == i] for i in np.unique(x_direction_)]

position = 0

for item in x_groups:
    x_avg_5.append(np.mean(x_groups[position]))
    b_avg_5.append(np.mean(b_groups[position]))
    z_avg_5.append(np.mean(z_groups[position]))
    position=position+1

J_x = []
for value in b_avg_5:
    j = value*2/(4*3.14*(10**7))
    J_x.append(j)

plt.title('average Current Density over x, 5kHz', fontsize=15)
plt.scatter(x_avg_5, J_x, color='teal',s=15, marker='*',label="b field")
plt.xlabel('X Position')
plt.ylabel('J(x)')
plt.show()
```

To find the maximums of each side of the apparatus:

```
print('Max value on left of 5k is:',np.array(b_avg_5[0:500]).max())
```

```
print('Max value on left of 250 is:',np.array(b_avg_250[0:200]).max())
print('Max value on right of 5k is:',np.array(b_avg_5[200:1000]).max())
print('Max value on right of 250 is:',np.array(b_avg_250[500:1000]).max())

a = [MAX 5k L]/[MAX 5k R]
b = [MAX 250 L]/MAX 250 R]
print('ratio of max batman ears of 5k is:', a)
print("ratio of maxes of 250 is:", b)
print('difference of ratios is:', (b-a)/b*100, '%')
```

To find resistivity (m is resistivity):

```
import numpy as np
import matplotlib.pyplot as plt
from scipy.optimize import curve_fit

x_data=np.array([]) #distance
y_data=np.array([]) #avg voltage
y_errorbars=np.array([]) #std dev of the 3 voltages$

fig1=plt.figure(1)

def linear_function(x,a,b):
  return a*x+b

popt, pcov = curve_fit(linear_function, x_data, y_data)
a_optimal, b_optimal = popt
```

```
y_fit = linear_function(x_data, a_optimal, b_optimal)

a_error, b_error = np.sqrt(np.diag(pcov))

plt.plot(x_data, y_data, 'blue', linestyle='none', marker='o', markerfacecolor='bl
plt.title('Avg Voltage [mV] vs Distance [cm]', fontsize=15)

$plt.ylabel('Avg Voltage [mV]', fontsize=15)
plt.yticks(size=15)

plt.xlabel('Distance [cm]', fontsize=15)
plt.xticks(size=15)

plt.plot(x_data, y_fit, label='Fitted Line', color='red')
plt.errorbar(x_data, y_data, y_errorbars, fmt='o', ecolor='black', capsize=7)

print("m:", a_optimal, "+/-", a_error)
print("b:", b_optimal, "+/-", b_error)
print("standard deviations:",y_errorbars)

fig1.show()
```

Bibliography

[1] Anne Blackwell, Andrew Rotunno (2019) *Demonstration of Lateral Skin Effect using a pick-up Coil*, John Essick, American Journal of Physics

[2] S. Du, William Mihara, Seth Aubin (2022) *Suppressing of potential roughness in atom chip ac Zeeman Traps*, PHYSICAL REVIEW A 105, 053127